ISTANBUL TECHNICAL UNIVERSITY ★ GRADUATE SCHOOL

EXPERIMENTAL INVESTIGATION OF LEADING EDGE SUCTION PARAMETER ON MASSIVELY SEPARATED FLOW

M.Sc. THESIS

Egemen AYDIN

Department of Aeronautics and Astronautics Engineering

Aeronautics and Astronautics Engineering Programme

MAY 2021

ISTANBUL TECHNICAL UNIVERSITY ★ GRADUATE SCHOOL

EXPERIMENTAL INVESTIGATION OF LEADING EDGE SUCTION PARAMETER ON MASSIVELY SEPARATED FLOW

M.Sc. THESIS

Egemen AYDIN
(511171150)

Department of Aeronautics & Astronautics Engineering

Aeronautics & Astronautics Engineering Programme

Thesis Advisor: Prof. Dr. Nuriye Leman Okşan ÇETİNER YILDIRIM

MAY 2021

ISTANBUL TEKNİK ÜNİVERSİTESİ ★ LİSANSÜSTÜ EĞİTİM ENSTİTÜSÜ

HUCUM KENARI EMME PARAMETRESININ SIDDETLI AYRIK AKIŞTA DENEYSEL INCELENMESI

YÜKSEK LİSANS TEZİ

Egemen AYDIN
(511171150)

Uçak ve Uzay Mühendisliği Anabilim Dalı

Uçak ve Uzay Mühendisliği Programı

Tez Danışmanı: Prof. Dr. Nuriye Leman Okşan ÇETİNER YILDIRIM

MAYIS 2021

Egemen Aydın, a M.Sc. student of ITU Graduate School student ID 511171150, successfully defended the thesis entitled "EXPERIMENTAL INVESTIGATION OF LEADING EDGE SUCTION PARAMETER ON MASSIVELY SEPARATED FLOW", which he prepared after fulfilling the requirements specified in the associated legislations, before the jury whose signatures are below.

Thesis Advisor :	**Prof. Dr. Okşan Çetiner Yıldırım** Istanbul Technical University	.....
Jury Members :	**Prof. Dr. Fırat Oğuz Edis** Istanbul Technical University	.....
	Assist. Prof. Sedat Tokgöz Gebze Technical University	.....

Date of Submission : 5 May 2021
Date of Defense : 10 May 2021

To my love,

FOREWORD

First of all, I would like to express my gratefulness to Trisonic Family. My thesis advisor Prof. Dr. N. L. Okşan Çetiner Yıldırım for her continous support and guidance during the development of this thesis and to Murat Sarıtaş, Onur Son, İdil Fenercioğlu, Hasan Tabanlı and Aliosman Tabanlı for their support and friendship.

I am also thankful to my friends for their valuable friendship and support. But most importantly, helping me against all the negativeness and stress of my school years.

And the last, I would like to express my gratitude to my family for their great support and encouragements. I would not be able to be at where I am without their love, efforts and guidance.

May 2021 Egemen AYDIN

TABLE OF CONTENTS

Page

FOREWORD ..... **ix**
TABLE OF CONTENTS ..... **xi**
ABBREVIATIONS ..... **xiii**
SYMBOLS ..... **xv**
LIST OF TABLES ..... **xvii**
LIST OF FIGURES ..... **xix**
SUMMARY ..... **xxi**
ÖZET…… ..... **xxiii**
1. INTRODUCTION **1**
2. STATE OF ART **3**
2.1 Thin Airfoil Theory 3
2.2 Leading Edge Suction 4
3. EXPERIMENTAL SETUP **7**
3.1 Flow System 7
3.2 Test Model 8
3.3 Force Measurement 9
3.4 Quantative Flow Visulation 9
4. RESULTS **11**
4.1 Experiment Basis and Selected Test Cases 11
4.2 LESP Parameter Derivation and Critical LESP Number 14
4.3 Flow Structures and LESP Parameter 15
6. CONCLUSIONS AND FUTURE WORK **23**
REFERENCES **25**
CURRICULUM VITAE **29**

ABBREVIATIONS

AoA **:** Angle of Attack

DPIV **:** Digital Partical Image Velocimetry

MAV **:** Micro Aerial Vehicle

Re **:** Reynolds Number

LESP **:** Leading Edge Suction Parameter

SYMBOLS

C_d	**:** Drag Coefficient
C_l	**:** Lift Coefficient
t	**:** Time
t^*	**:** Convective time
α	**:** Angle of attack
Re	**:** Reynolds number
U_∞	**:** Freestream Velocity
c	**:** Wing chord
C_S	**:** Leading edge suction force coefficent
A_0	**:** First fourier coefficent of thin airfoil theory

LIST OF TABLES

Page

Table 4.1 : Selected Test Cases ……...……**14**
Table 4.2 : Force graph and the DPIV images of experiment 1……...……**17**
Table 4.3 : Force graph and the DPIV images of experiment 3……...……**19**
Table 4.4 : Force graph and the DPIV images of experiment 5……...……**21**

LIST OF FIGURES

Page

Figure 2.1 : Stagnation point and the flow around the leading edge [3]……5
Figure 3.1 : Schematics of water channel [19]……...8
Figure 3.2 : Schematics of experimental setup……...9
Figure 4.1 : Angle of attack changes in time……11
Figure 4.2 : Vertical offset of the test model from the gust generator plane…….12
Figure 4.3 : PIV images of Offset=29 mm, AoA=20°……...13

EXPERIMENTAL INVESTIGATION OF LEADING EDGE SUCTION PARAMETER ON MASSIVELY SEPARATED FLOW

SUMMARY

The study aims to investigate and understand the Leading Edge Suction Parameter (LESP) application on the massively separated flow. The experiment was done by gathering force data from the downstream flat plate and the visualization of the flow structures is done by Digital Particle Image Velocimetry.

The experiments are conducted in free surface, closed-circuit, large scale water channel located in Trisonic Laboratory of Istanbul Technical University's Faculty of Aeronautics and Astronautics. The velocity of the tunnel is equal to 0.1 m/s which results in a 10.000 Reynolds Number. During the experiment, the flat plate at the downstream of the gust generator (plat plate) is kept constant angle of attack and the test cases are selecting to show that the LESP parameter that derived from only one force component works for different gust interaction with the flat plate. As already discussed in the literature, the critical LESP parameter depends on only airfoil shape and its ambient Reynolds Number. Also, the critical LESP number is calculated in literature as equal to 0,05 for plat plate at the 10,000 Reynolds Number. We did not perform an experiment to find critical LEPS numbers as our experiment was done with a flat plate on 10,000 Re.

A different angle of attack and different gust impingement combination has been shown that the LESP parameter works even in a highly unstable gust environment. Flow structures around the airfoil leading edge are behaving as expected from the LESP theory (leading-edge vortex separation and unification).

HUCUM KENARI EMME PARAMETRESININ SIDDETLI AYRIK AKIŞTA DENEYSEL INCELENMESI

ÖZET

Çalışmanın amacı, stabil olmayan sağanak akışında hücum kenar emme parametresi uygulamasını araştırmak ve anlamaktır. Akış yönündeki düz plakadan kuvvet verileri toplandı ve akış yapılarının görselleştirilmesi için Dijital Parçacık Görüntü Hız Ölçümü kullanıldı.

Mevcut havacılık araştırmalarının geniş uygulama yelpazesi şüphesiz kararsız akış fenomenlerini içerir. Küçük boyutları ve düşük hız gereksinimleri nedeniyle yaygın bir örnek mikro hava aracı olarak düşünülebilir; ayrıca doğadan da böcek uçuşları benzer bir örnek olarak gösterilebilir. Böcekler, uçma eylemini başarmak için yüksek hareket hızlarıyla kanat çırpma hareketleri yapmaktadır. Böcek uçuşunun aerodinamik fenomeninin anlaşılması, daha çok arzu edilen yüksek manevra kabiliyetine sahip mikro hava taşıtlarının elde edilmesi yolunda inkâr edilemeyecek kadar önemlidir.

Böcek uçuşundaki hücum açısındaki ve hızındaki büyük değişlikler karmaşık kararsız akışları içermekte ve hem hücum açısı hem de hızdaki bu büyük farklılıklar dinamik stall oluşumuna neden olabilmektedirler. Dinamik stall'ın en etkili özelliklerinden biri, kanat profilinin hücum açısı statik stall açısını aştığında, büyük ölçekli dinamik girdap kanat profilinden ayrılırken meydana gelmesidir. Bu dinamik girdap oluşumu, kanadın kaldırma kuvveti geçmişini değiştirirken anlık yüksek genlikli değişikliklere neden olabilmektedir. Dinamik stall yapının yaşam döngüsünü kısaltırken aracın performansını etkileyebilecek yüksek aerodinamik yükler veya tehlikeli titreşimler oluşturabilir. Bu nedenle, sistemin güvenliğini sağlamak için dinamik stall durumundan kaçınılır; ancak bunun tersine, böcek uçuşundaki hücum kenarı girdapları, kanat çırpma uçuşunun başarısından sorumlu en önemli parametre olarak literatürde gösterilmiştir. Bu girdaplara ek olarak, mikro hava taşıtları atmosferik türbülanslara da oldukça maruz kalmaktadır ve bu dalgalanmalar, oldukça çevik olması beklenen araçlarda kontrol zorluklarına neden olabilmektedir. Mikro hava araçlarının tasarımında, manevra kabiliyeti ve sabit uçuş koşullarını sürdürme yeteneği güçlü bir etkiye sahiptir.

Hücum kenarı girdap parametreleri, dinamik stall'ın başlamasıyla ilişkilendirilmiştir ve dinamik stall oluşumu, Fourier serisinin ince-kanat teorisindeki ilk terimi ile ilişkilendirilmiştir. Kanat hücum kenarındaki emme gücü, hücum kenar hızı ile orantılı bir ilişkiye sahiptir ve bu emme parametresi, ön kenar girdap oluşumunun başlatma kriterleri için kullanılmıştır.

Ramesh vd. bir girdap parçalandığında hücum kenarında ortaya çıkan emiş parametresi için ince kanat teorisi Fourier serisinin ilk teriminin kritik bir eşik sayısının olduğu gözlemlendi ve bu nicel sayı hücum kenarı emme parametresi (LESP) olarak adlandırıldı. Bu fikir, kanat profilinin belirli bir miktar emiş miktarını destekleyebileceği düşüncesine dayanmaktadır. Bu sınır aşılırsa, girdap hücum kenarından serbest bırakılır ve dinamik stall ile hücum kenar girdabı oluşur. Kritik LESP değeri, kanat şekline ve Reynolds sayısına bağlıdır ancak hareket kinematiğinden bağımsızdır. LESP çalışmaları, deneysel kuvvet ölçümünden parametrenin hesaplanmasıyla başlamış, ardından fenomeni anlamak ve parametrenin akış için dinamik bir modele uygulanması için CFD çözümleri kullanılmıştır. Parametrenin bilinmesinden sonra, potansiyel kullanım alanlarını ve parametrenin sınırlarını keşfetmek için diğer araştırmacılar tarafından literatüre önemli ölçüde çaba gösterilmiştir.

Deneyler serbest yüzey, kapalı devre, büyük ölçekli su kanalında yapıldı. Kanal İstanbul Teknik Üniversitesi Uçak ve Uzay Fakültesi Trisonik Laboratuvarı'nda bulunmaktadır. Tünelin hızı 0.1 m/s 'ye eşittir ve bu da aynı zamanda 10.000 Reynolds Sayısına denk gelmektedir. Deney sırasında, sağanak üretecinin akış aşağısındaki düz plaka sabit hücum açısında tutulur ve test seçenekleri, yalnızca bir kuvvet bileşeninden türetilen LESP parametresinin farklı sağanak etkileşimi için çalıştığını göstermek için seçildi. Ayrıca literatürde kritik LESP sayısı düz plaka için 10.000 Reynolds sayısında 0,05'e eşit olarak hesaplanmıştır. Deney 10.000 Reynolds sayısında da düz plaka ile yapıldığından kritik LEPS numarasını bulmak için ayrıca bir deney yapılmasına gerek kalmadı.

Bu çalışmada, LESP hipotezi, büyük ölçüde ayrılmış bir sağanak akış ortamında araştırılmış ve LESP parametresi, kuvvet sensörünün y vektörünün bir fonksiyonu olarak hesaplanmıştır. Farklı bir hücum açısı ve farklı fırtına çarpma kombinasyonlarının, LESP parametresinin oldukça dengesiz sağanak ortamında bile çalıştığı gösterilmiştir. Kenar hücum kenarı etrafındaki akış yapıları dijital parçacık

görüntü hız ölçümü sistemi tarafından görüntülendi ve kuvvet sensörü eşzamanlı olarak kuvvetleri topladı. Sonuç olarak düz plaka etrafındaki akış yapılarının, hücum kenarı girdaplarının ayırma ve birleştirme hareketlerinin LESP teorisinden beklendiği gibi davrandığını gösterilmiştir.

1. INTRODUCTION

A wide range of applications of current aerospace research undoubtedly includes unsteady flow phenomena in nearly every aspect. Common examples can be listed to application areas such as rotorcraft, delta wing, wind turbine aerodynamics as well as micro air vehicles (MAV) but not limited.

Small size and low-speed requirements of the MAV's lead to a low Reynolds number regime and high dimensionless rates of motion that insect flies can be shown as an example from nature. They set in motion of flapping flight with high dimensionless rates of motion to achieve an act of flying; consequently, the understand the aerodynamic phenomena of the insect flight is undeniably crucial on the path of the achieve more desirable highly maneuverable MAV's.

The large fluctuation on the angle of attack with the large incident velocity of the insect flight could be connected to the complex unsteady flows. These large variations on both angle of attack and velocity might lead to the undesirable event of dynamic stall. The time-dependent event of unsteady flow separation on the wing or airfoil is named a dynamic stall in literature. One of the influential characteristics of the dynamic stall happens when the airfoil angle of attack exceeds the static stall angle as the large-scale dynamic vortex shedding from the airfoil. This dynamic vortex occurrence could cause an overshoot on the lift while altering the lift history. High aerodynamic loads or dangerous vibrations could happen on the dynamic stall phase which may affect the performance of the vehicle while shortening the life cycle of the structure. Hence, it is desirable to eliminate the effect of the dynamic stall to ensure the safety reliability of the system; however, on the contrary, Leading Edge Vortices (LEV) pinpointed as the oe of the most important parameter for the success of flapping flight in insect flight [1–4].

Small-amplitude unsteady flows have been inestigated broadly by researchers such as Theodorsen [5] and Wagner [6]. Also, the rotorcraft community tried to develop methods of studying LEVs because of the dynamic stall encounterings [7,8]. Several semi-empirical methods have been established to use in rotor design yet some of the

model the effect of the leading-edge vortices on the flow field and the forces; however, all of these methods do not take into account the condition where or when the leading-edge vortices initiated.

The flow parameters of the leading edge had been associated with the initiation of the dynamic stall [9]. Stall occurrence is also associated with the first term A_0 of the Fourier's series in thin-airfoil theory [10]. As expected, the strength of the suction peak has proportional relation with the velocity of the leading edge [11], and these suction parameters have been used for the initiation criteria of the leading-edge vortex formation [12].

Ramesh et al. observed that there is a critical threshold number of the first term of the Fourier series for the leading-edge suction when a vortex is being shredded [13]. They named this number, A_0, as the leading-edge suction parameter (LESP). This idea is based on the thought that airfoil could maintain a certain amount of leading-edge suction. If this threshold is exceeded, leading edge vorticity is released from the leading edge and set a dynamic stall. According to Ramesh, the decisive LESP value depends on the airfoil shape and the Reynolds number but independent of the motion kinematics.

In this thesis, we investigated the time variant of force measurement of the airfoil with the PIV images for the experimental evidence of a critical leading-edge suction parameter. The change of LESP values until the separation (critical LESP value) has been investigated for different gust impingements on a flat plate.

2. STATE OF ART

2.1 Thin Airfoil Theory

The thin-Airfoil theory state that the airfoil could be modeled by a vortex sheet ($\gamma(x,t)$) along the chord line in a uniform flow (V_∞).

In theory, the camber line must be the streamline of this flow and from this condition, the strength of the vortexes on the chord is determined. This occurrence leads the singular integral equations as below from Bio-Savart Law;

$$\frac{1}{2\pi}\oint_0^c \frac{\gamma(\xi)d\xi}{x-\xi} = V_\infty\left[\alpha - \left(\frac{dz}{dx}\right)\right] \tag{2.1}$$

Where;

$$x = \frac{c}{2}(1-\cos\theta_0) \tag{2.2}$$

$$\xi = \frac{c}{2}(1-cos\,\theta) \tag{2.3}$$

X indicates the location where induced velocity is generated and ξ indicates the location where vortexes produce the velocity. c is the airfoil chord and θ varies from 0 to π as x varies from 0 to 1 along the airfoil

When substitute equation 2.2 and 2.3 into equation 2.1, we get;

$$\frac{1}{2\pi}\oint_0^\pi \frac{\gamma(\theta,t)\sin\theta d\theta}{\cos\theta-\cos\theta_0} = U_\infty\left[\alpha - \left(\frac{dz}{dx}\right)\right] \tag{2.4}$$

The Fourier expansion of the vortex sheet from equation 2.4 leads to

$$\gamma(\theta) = 2U\left(A_0\frac{1+\cos\theta}{\sin\theta} + \sum_{n=1}^{\infty} A_n \sin n\theta\right) \tag{2.5}$$

Where A_n coefficients with A_0 are Fourier coefficients and these constants could be found from in terms of the slope of the camber line dz/dx and the angle of attack α the Fourier coefficients can be presented in terms of the local downwash $W(x,t)$ as

$$A_0(t) = -\frac{1}{\pi}\int_0^{\pi} \frac{W(x,t)}{U(t)} d\theta \tag{2.6}$$

$$A_n(t) = \frac{2}{\pi}\int_0^{\pi} \frac{W(x,t)}{U(t)} cos\, n\theta\, d\theta \tag{2.7}$$

$W(x,t)$ is the instantaneous chordwise downwash on the airfoil.

The local downwash could be establish by applying the boundary conditions of the Kutta condition and perpendicular flow through the airfoil surface. This is a function of the airfoil motion kinematics as well as shed-vortex history.

There are two main forces acting on the airfoil and these are respectively the normal force and the leading-edge suction force. These two force coefficients could be derived from Fourier coefficients such as;

$$C_N = 2\pi\left[\left(\cos\alpha + \frac{\dot{h}}{U} sin\alpha\right)\left(A_0 + \frac{A_1}{2}\right) + \left(\frac{c}{U^2}\right)\left(\frac{3}{4}\frac{\partial}{\partial t}(UA_0) + \frac{1}{4}\frac{\partial}{\partial t}(UA_1) + \frac{1}{8}\frac{\partial}{\partial t}(UA_2)\right)\right] \tag{2.8}$$

$$C_S = 2\pi A_0^2 \tag{2.9}$$

2.2 Leading Edge Suction

From the inviscid flow theory of an infinitely-thin flat plate, it can be seen that pressure could supposedly only cause a force perpendicular to the plate. However, this paradox is resolved by the Kutta condition which states the velocity at the leading edge remnant infinite. Consequently, the pressure becomes negatively infinite, and pressure's integral over the leading edge results in a finite suction vector that parallel to the plate [14]. This force occurrence is named as leading-edge suction force and the remainder normal force on the flat plate is equal to the Kutta–Joukowski lift.

Figure 2.1: Stagnation point and the flow around the leading edge.[3]

For the attached flow condition, the flow tries to go from the stagnation point which is located on the lower surface of the airfoil to the top surface of the airfoil while accelerated around the leading edge. As expected, pressure is required to rebalance the centrifugal force created by the flow around the leading edge and this occurrence leads to leading edge suction force. But as the airfoil thickness approaches zero, the flow seeks the way that goes exactly 180° upward at the leading edge [18]. This leads to the theoretically infinite velocity at the leading edge. The formula of the theoretically infinite velocity is provided by Garrick [16] and von Kármán & Burgers [17] as;

$$V_{LE}(t) = \frac{1}{2}\log_{x\to LE}\gamma(x,t)\sqrt{x} \tag{2.10}$$

Using the vorticity distribution from the thin airfoil theory (formula 5);

$$V_{LE}(t) = \log_{x\to 0^+}U(t)A_0(t)\frac{1+\cos\theta}{\sin\theta}\sqrt{\frac{1}{2}(1-\cos\theta)}\ (11) \tag{2.11}$$

$$V_{LE}(t) = \log_{x\to 0^+}U(t)A_0(t)\sqrt{\frac{c}{2}(1+\cos\theta)}\ (12) \tag{2.12}$$

$$V_{LE}(t) = \sqrt{c}U(t)A_0(t)\ (13) \tag{2.13}$$

The Leading-Edge Suction Parameter (LESP) [13] is determined by nondimensionalizing the leading-edge velocity with the freestream velocity. The formulation becomes;

$$LESP(t) = A_0(t) \tag{2.14}$$

The velocity at the leading-edge and the Leading Edge Suction Parameter (LESP) is obtained from the first Fourier term coefficient of vortex sheet equation from thin airfoil theory (A_0). Ramesh's [11] theory is that there is a decisive threshold number for LESP for given Reynolds number and airfoil shape, which determines whether the flow is separated or not at the leading-edge of the airfoil. Ramesh [11] also stated that this parameter works for any kinematic motion and Reynolds number.

For the suction side of the airfoil while the LESP is increasing, the separation take place when it pass over the critical threshold value. On the contrary, while the LESP is decreasing, the flow at the leading edge becomes fully attached as it pass the critical threshold value. The negative of LESP demonstrate whether the flow is separated or not on the pressure side of the airfoil [11].

As it mentiond before, two main forces acting on the airfoil are the normal force and the leading-edge suction force (Eqs. 8 and 9). The lift and drag coefficients in terms of these two forces are ;

$$C_l = C_N \cos\theta + C_S \sin\theta \tag{2.15}$$

$$C_d = C_N \sin\theta - C_S \cos\theta \tag{2.16}$$

In the above formulation, the vector summation of the terms without the time derivative in the normal force and the leading-edge suction force are equal to the total circulatory force. the terms containing the time derivative in the normal force consist of the apparent mass force. Consequently, the apparent-mass force is in the normal direction and it contributes to lift as well as drag.[15]

3. EXPERIMENTAL SETUP

The experimental set-up is made of the flow system (the water channel), model, and the experimental apparatus (the cameras, lasers, the PIV, and direct force and torque measurement system).

3.1 Flow System

The experiments are done in closed circuit, free surface, large scale water channel in Trisonic Laboratory of Istanbul Technical University's Faculty of Aeronautics and Astronautics. The water has several parts to provide better flow conditions for experiments. Firstly, regular city system water goes through carbon and propylene sediment filters for decontamination which is important to get better results on the DPIV system. Then secondly, the centrifugal pump system directs the water to settling chamber. Just before in the test section, honeycomb structures and screen arrangements decrease the turbulent intensity of the water. After this process, water accelerated into the test section with 2:1 contraction. The test section is purposely made of transparent glass to allow the laser beams of the DPIV measurement system. The dimensions of the test section are 1010 mm to 790 mm. A detailed description of the flow facility is given in [20, 21].

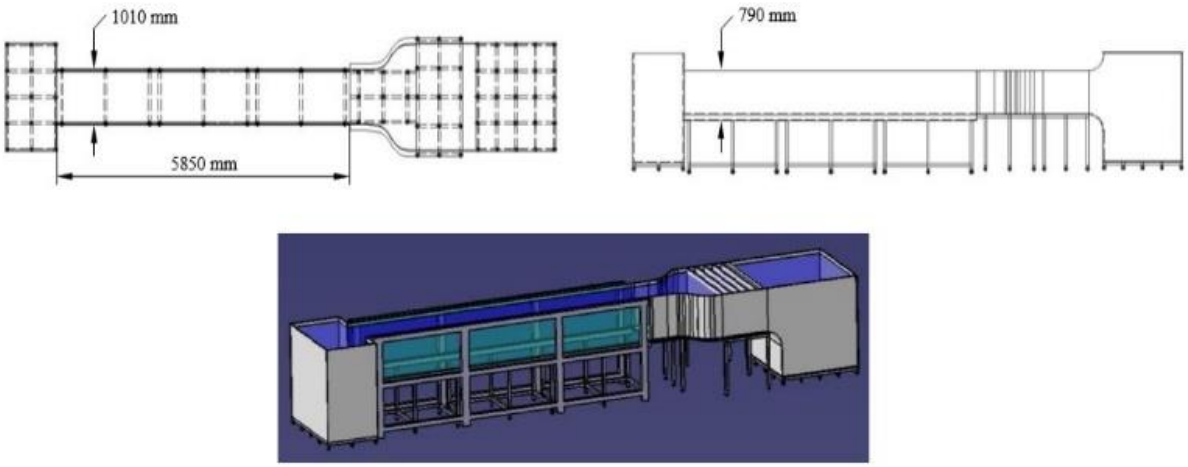

Figure 3.1 : Schematics of water channel [19]

3.2 Test Model

A flat plate that has a 10cm chord and 40cm span is used as a gust generator and it is mounted from its mid-chord. Another flat plate with a 10cm chord and 20cm span (half aspect ratio of gust generator) was used to examine the effect of the vortex generated from the upstream flat plate and it is mounted from its leading edge. The two flat plates are manufactured from plexiglass to allow DPIV lasers go-though. Experimental setup visualization can be seen in Figure 3.2.

Mounting beams of the flat plates are connected to pitch motors also are connected to the linear tables. A pitch motor is used to change the angle of attack of the model and the linear tables are used to give plunge motion. These motors can be worked simultaneously.

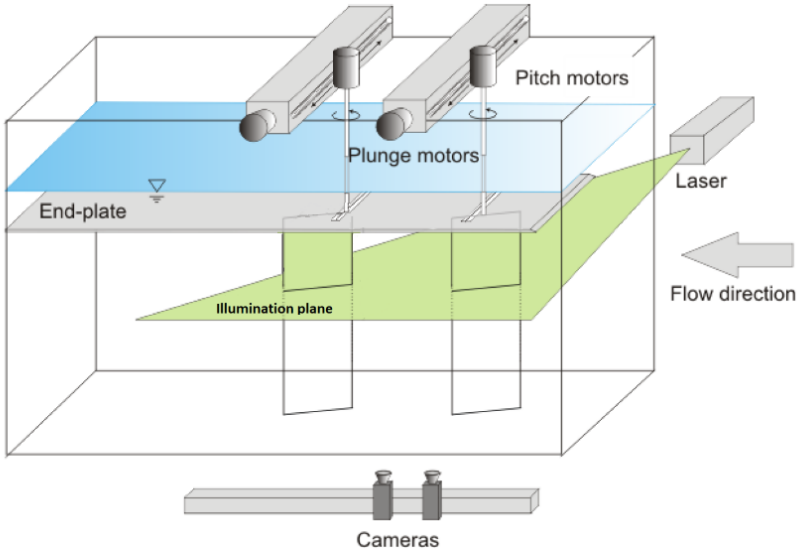

Figure 3.2 : Schematics of experimental setup

3.3 Force Measurement

The force/torque sensors are attached to the mounting beam. For 3-axis force and 3-axis moment measurements, the ATI NANO-17 IP68 Force/Torque sensor is used. A LabVIEW VI is used the control the movements of the model by adjusting synchronization with DPIV and force torque measurements of the sensor.

Sensor data acquisition has a 1000Hz sampling rate and FFT low pass filter is used to eliminate mechanical vibrations and noises. The cut-off frequency is chosen by considering the motion of the gust generator to not eliminate the source of the disturbance. Gust generator flat plate motion continues in 4 seconds which equal to 0.25 Hz in cyclic case. The cut-off frequency for the FFT is taken 5 times the frequency of the gust generator which is equal to 1.25 Hz.

3.4 Quantative Flow Visulation

The DPIV (Digital Particle Image Velocimetry) system with Dynamic Studio software (Dantec Dynamics A/S) is used in the test section of the channel to record flow fields around and in the wake of the wing and flap. The flow is illuminated by a dual cavity Nd:Yag laser with a maximum of 120 mJpulse at a wavelength of 532 nm. The flow

is seeded polyamide particles with a mean diameter of 50μm. As it can be seen on the left side of figure 3.2, the light-sheet plane was located at plates half-span and the velocity fields around the wake of the plate are captured by using two 10bit Dantec Dynamics Flow Sense 2M CCD cameras with 1600 x 1200 pixels resolution, positioned underneath the water channel to obtain velocity flow fields. Each experimental data set included 230 images. The PIV images were interrogated using an cross correlation technique with an interrogation size of 16x16 pixels and it has %50 overlap in each direction.

4. RESULTS

In this section, all the results will be provided with dimensional time, however, it should be kept in mind that the convective time is equal to the dimensional time as the chord length give the same time in second in all of the experiments.

The provided experiment results are scrutinized before in the MSc thesis of the Kader Engin [22] in detail in terms of gust characterization, observation on force data (specifically lift and drag changes), and effects on the flow structures. However, in this thesis the same experimental data set is used only for the understand and the show that the LESP parameter on the unsteady flow like on gust environment. For the sake of simplicity, all the experimental cases will not be provided in this thesis.

4.1 Experiment Basis and Selected Test Cases

During the experiment, the flat plate at the downstream of gust generator (another plat plate) is kept constant angle of attack. The gust generator performs a ramp motion in pitching stating at t=5s to t=9s while protecting its angular velocity of 45 degrees per second. Figure 4.1 shows the angle of attack change of the gust generator in time.

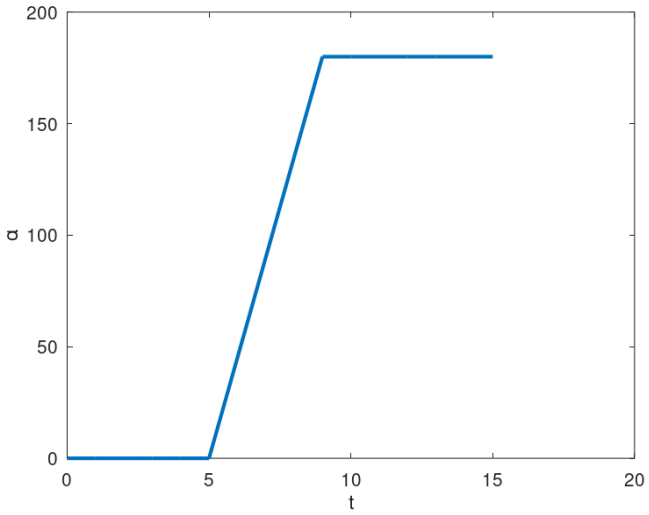

Figure 4.1: Angle of attack changes in time

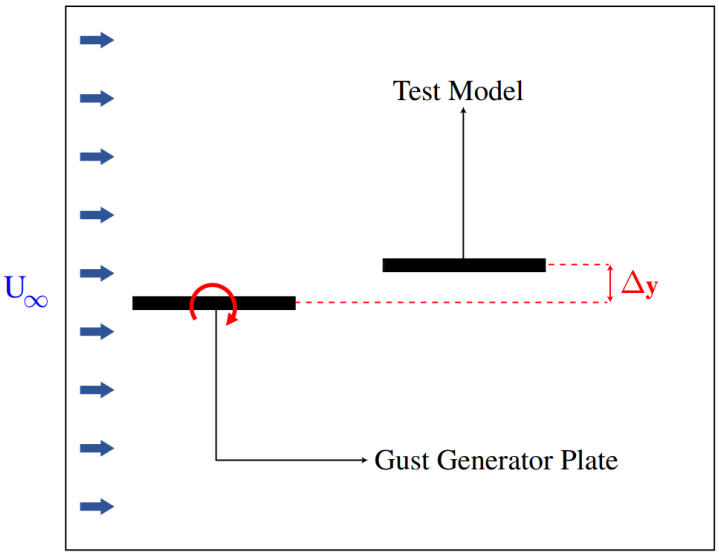

Figure 4.2: Vertical offset of the test model from the gust generator plane

The vertical distance (y-coordinate) between the flat plate at the downstream and the gust generator is named as an offset and there 3 different experimental cases done with different offset which are 19mm, 29mm, and 39mm as it shown in Figure 4.2. Also, there are 4 differents angle of attack combination of 0 deg, 10 deg 20 deg 45deg.

DPIV images to show how the experimental case looks like can be seen in figure 4.2. The first row of DPIV images in figure 4.2 shows the steady state before the gust generator starts its movement. The gust generator begins its motion on the first image of the second row and continues until the third row pf the last image. After this time point the effect of gust starting to disappear and the flow field starting to neutralize.

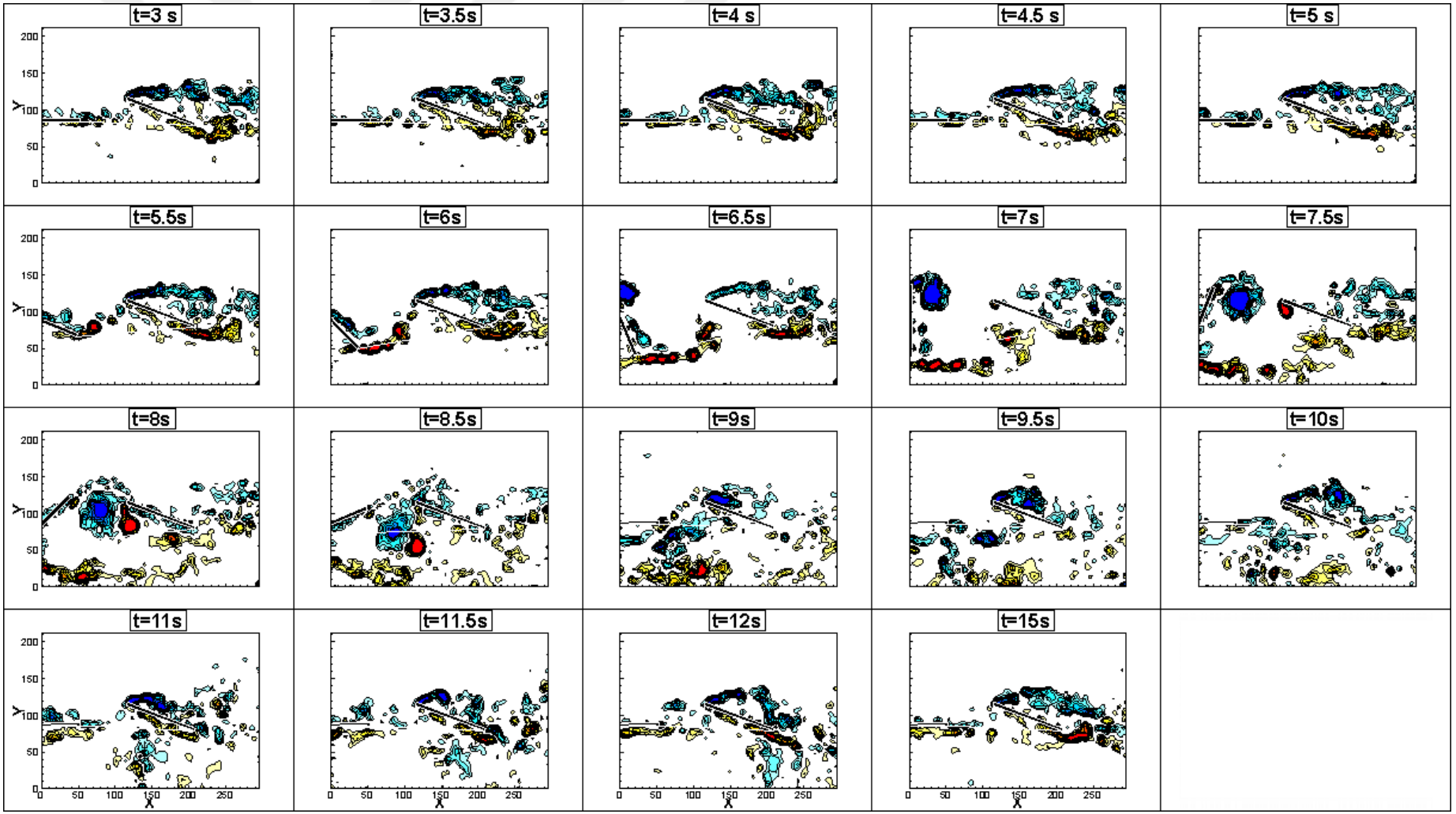

Figure 4.3 PIV images of Offset=29 mm, AoA=20°

Test cases are selecting to show that the LESP parameter that derived from only one force component (mathematical details provided in state of art section) works for different gust interaction with the flat plate. The LESP parameter changes on time with the down selected DPIV images will be provided accordingly. Table 4.1 shows the selected and investigated test cases and their parameters. Boldly written test cases are investigated in detail in this section.

Table 4.1: Selected test cases

Experiment no	Gust Generator	Model
	y- coordinate offset (mm)	AoA
1	**19**	**0**
2	19	20
3	**19**	**45**
4	29	0
5	**29**	**20**
6	39	0
7	39	45

4.2 LESP Parameter Derivation and Critical LESP Number

As stated in the state of the art section, the LESP parameter (A_0) is a function of suction force. Force measurements directions on the experiment from the flat plate respectively are perpendicular to the plate and parallel to the plate. Parallel vector measurement is equal to the suction force. With the help of equation 2.9, we calculated the LESP parameter as;

$$\sqrt{\frac{C_S}{2\pi}} = A_0 \tag{4.1}$$

But it is concluded that the LESP parameter could go negative values as the suction force go negative. Note that negative LESP demonstrate whether the flow is separated or not on the pressure side of the airfoil. Consequently, formula manipulated as.

$$If\ C_S \geq 0\ ;\ \sqrt{\frac{C_S}{2\pi}} = A_0 \tag{4.2}$$

$$If\ C_S\ < 0\ ; -\sqrt{\frac{-C_S}{2\pi}} = A_0 \tag{4.3}$$

LESP parameter changes with time calculated from the force measurement by using these two formulas.

As Ramesh explained in [13], the critical LESP parameter depends on only airfoil shape and its ambient Reynolds Number. Also, Ramesh calculates that the critical LESP number is equal to 0,05 for plat plate on the 10,000 Re. We did not perform an experiment to find critical LEPS numbers as our experiment was done with a flat plate on 10,000 Re. Also, the following results will show that this critical LESP parameter works perfectly fine in our experimental setup.

4.3 Flow Structures and LESP Parameter

Selected DPIV images show the evolution of the flow structures before and after the merge and the separation of the leading-edge vorticity on the flat plate. These image selections are made by looking at the intersection timepoints with the critical LESP number. However, because of the DPIV time resolution, the closest time points have been selected. Grey marks on the graph show the acquired DPIV images' timepoints and the black ones show the selected ones to represent flow structures.

Table 4.2 displays the 10 DPIV image and the flat plate's LESP number evolution on time. As can be seen on the graph in the first row, the LESP is greater than its LESP critical number of 0,05 at the beginning of the experiment. Then the parameter starts the drop while crossing the positive and the negative critical LESP number. After bottoming, it starts to increase again through the number that exceeds the positive critical number. Special to this case it touches positive critical LESP number again then increase again. Each of these intersections with the critical number will be explained in the following passages.

On the steady state phase of the experiment, as mentioned before, the LESP number is greater than its critical number. This occurrence could be seen on the first DPIV image as the vorticity on the leading edge is not on the flat plate completely.

On the second DPIV image time point, we are seeing that the gust generator starting to have an effect on the flow structures on the downstream plate. As the LESP parameter exceed the critical number, we are able to notice on the second DPIV image

that leading edge vorticity mildly seperated from the leading edge of the flat plate on the second one. Then on the way of the smaller LESP value, leading edge vorticity is again on the flat plate on the third PIV image.

LESP parameter starting decrease after the leading-edge vorticity merges with the flat plate on positive critical LESP number and even it goes to minus through to LESP critical number. Recall that the negative critical LESP number demonstrate whether the flow is separated or not on the pressure side of the airfoil and absolute values of the critical LESP numbers for the pressure side and suction side are equal to each other. The fourth DPIV image shows the exact time point where the LESP parameter of the flat plate equal to the negative critical number. We are able to see at that on that time point the counterclockwise vortex starting to build on the pressure side of the flat plate. After the creation of the counterclockwise vortex, the LESP parameter goes even more negative with the increasing power of the generated vortex on the plate. On the 5th image of the DPIV we are able to see that just before the clockwise vortex that came from the gust generator hits the plate, the counterclockwise vortex is still attached to the plate. The LESP number is useful between its positive and negative critical number. Beyond this range does not specifically mean anything on flow structures because the suction force direction starting to change after the separation [18]. Suction force direction change has been studied before by Deparday [23].

At the 6th DPIV image, the positive vortex has been freed itself from the plate nearly at the time point that where LESP parameter equal to the negative critical number again. Consequently, it is concluded that the direction of the LESP through the critical intersection is characterized by the flow structures on the airfoil. For example, on the time point 3, LESP was on the way to the negative values, negative slope, on that intersection, the counterrotating vortex started the built itself; however, on the time point 6, LESP was on the way to the positive values, positive slope, on that intersection the counterrotating vortex freed itself with separation.

After the counterclockwise rotating vortex is separated, LESP values jump to the positive critical number at a very fast pace. The clockwise rotating vortex is on the leading edge but it is about the separate as LESP equal to its critical number on the 7th DPIV image.

On the 8th DPIV image, the leading-edge vortices are separated from the flat plate as the LESP number is greater than 0,05. But suddenly, LESP goes to dive on the critical

number again as the leading edge vorticity sticks on the leading edge of the flat plate at the last DPIV image.

Table 4.2: Force graph and the DPIV images of experiment 1

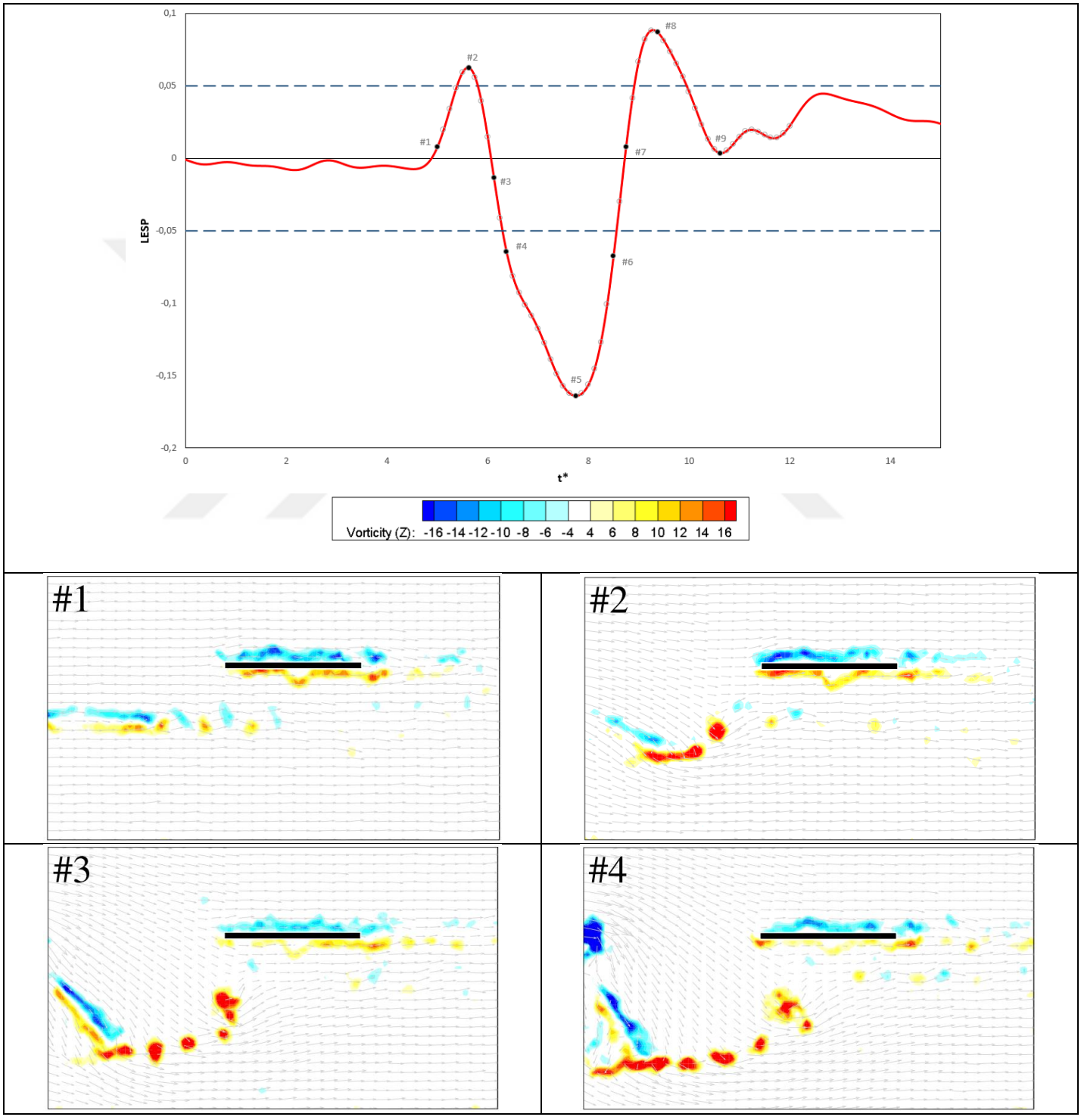

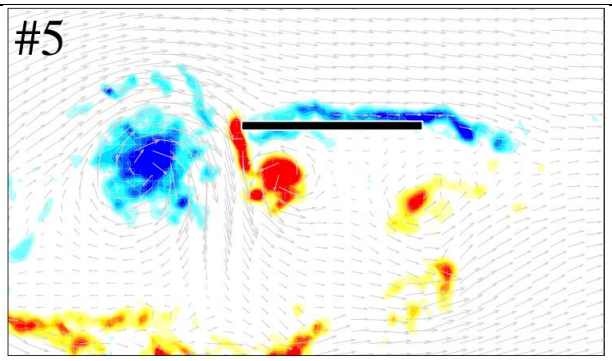

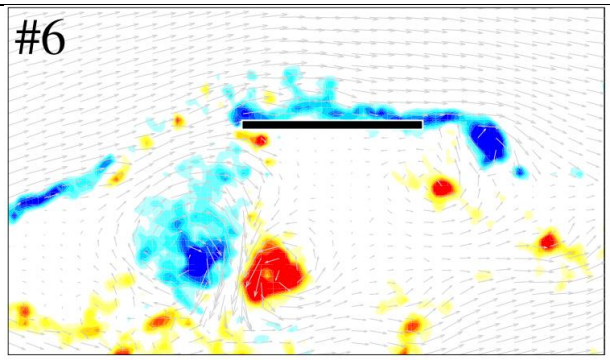

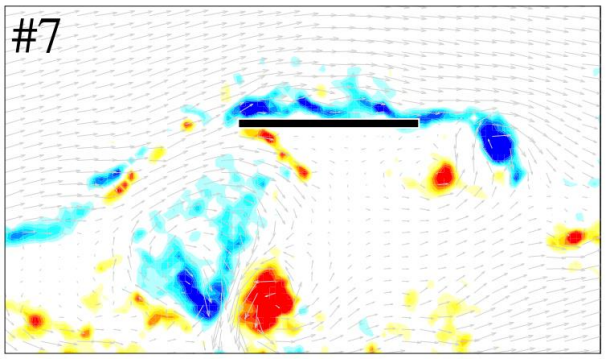

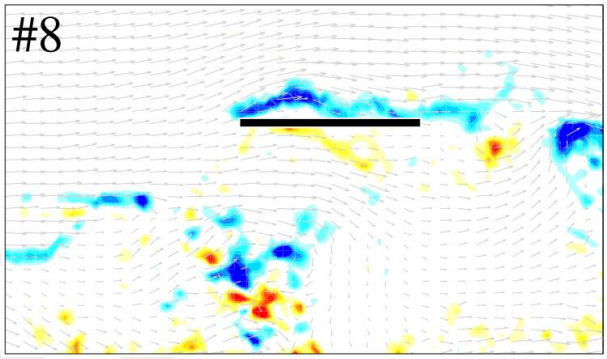

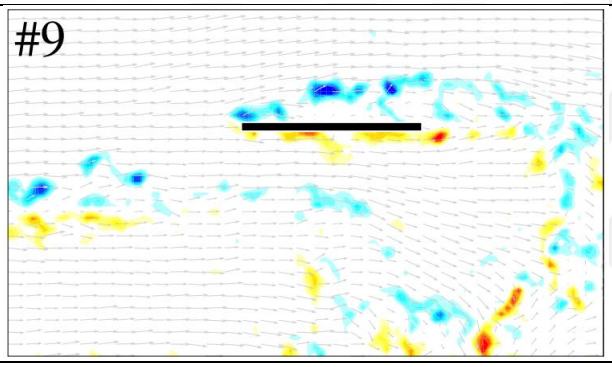

If we change the angle of attack of the flat plate while letting the gust generator same as in the previous experiment, the LESP parameter work as expected. The LESP number on steady state greater than it is a critical number means that the leading edge vortex is not on the flat plate and the first PIV images of table 4.3 clearly show that behaviour. At the third DPIV capture, there is no vorticity left on the leading edge of the flat plate as the LESP parameter below 0.05. At the fourth time point counterrotating vortex starting to build itself while reaching its peak strength on the fifth image. Respectively on the sixth PIV capture the counter rotating vortex freed itself from the airfoil, then the leading-edge vortex stick on the leading edge at a very minimal amount because of the gust effect. Finally, it returns to its original steady state separated leading edge vortex. In a summary changing the angle of attack did not

change nor critical LESP parameter or the vortex behavior on the between critical number region.

Table 4.3: Force graph and the DPIV images of experiment 3

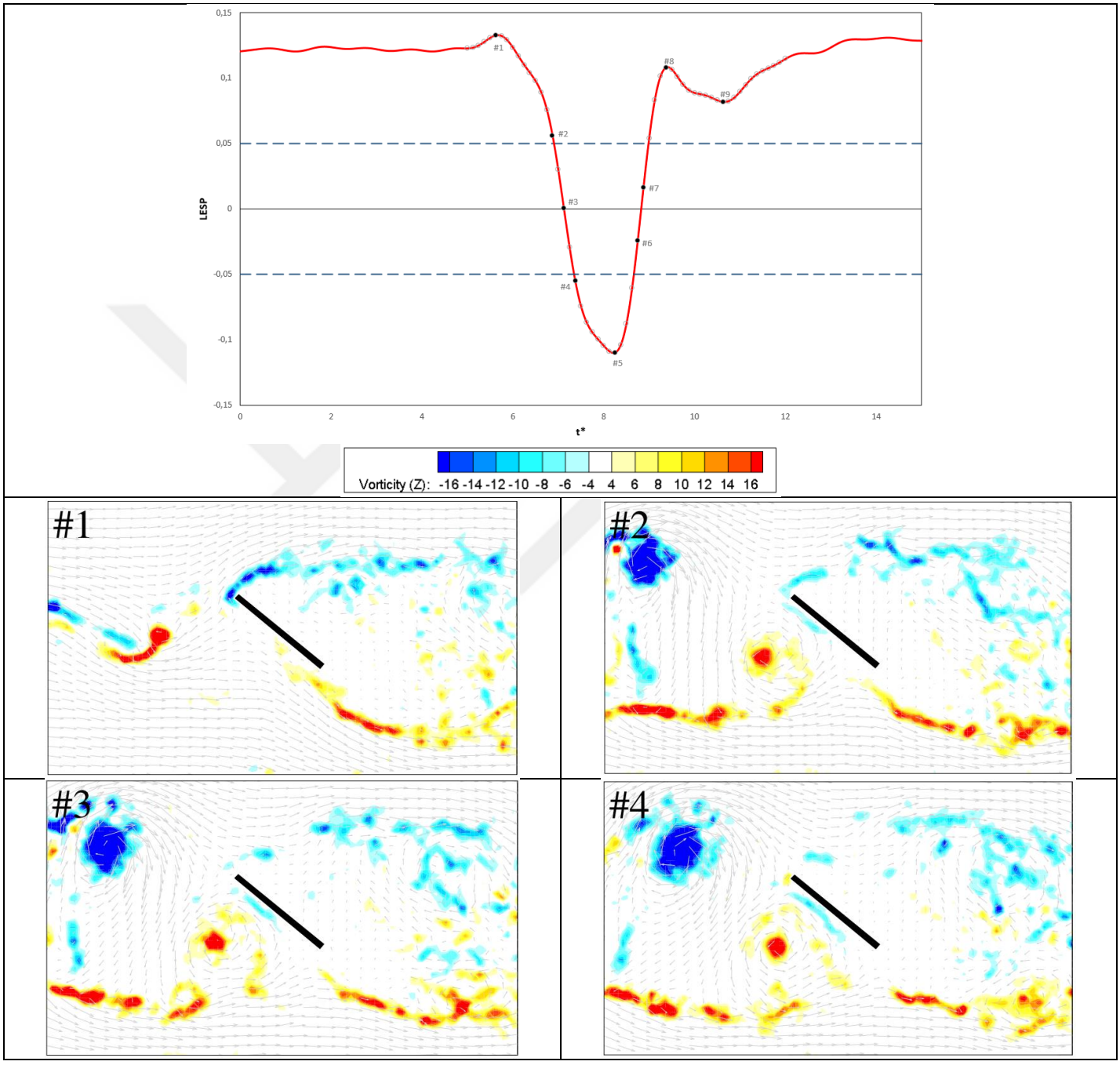

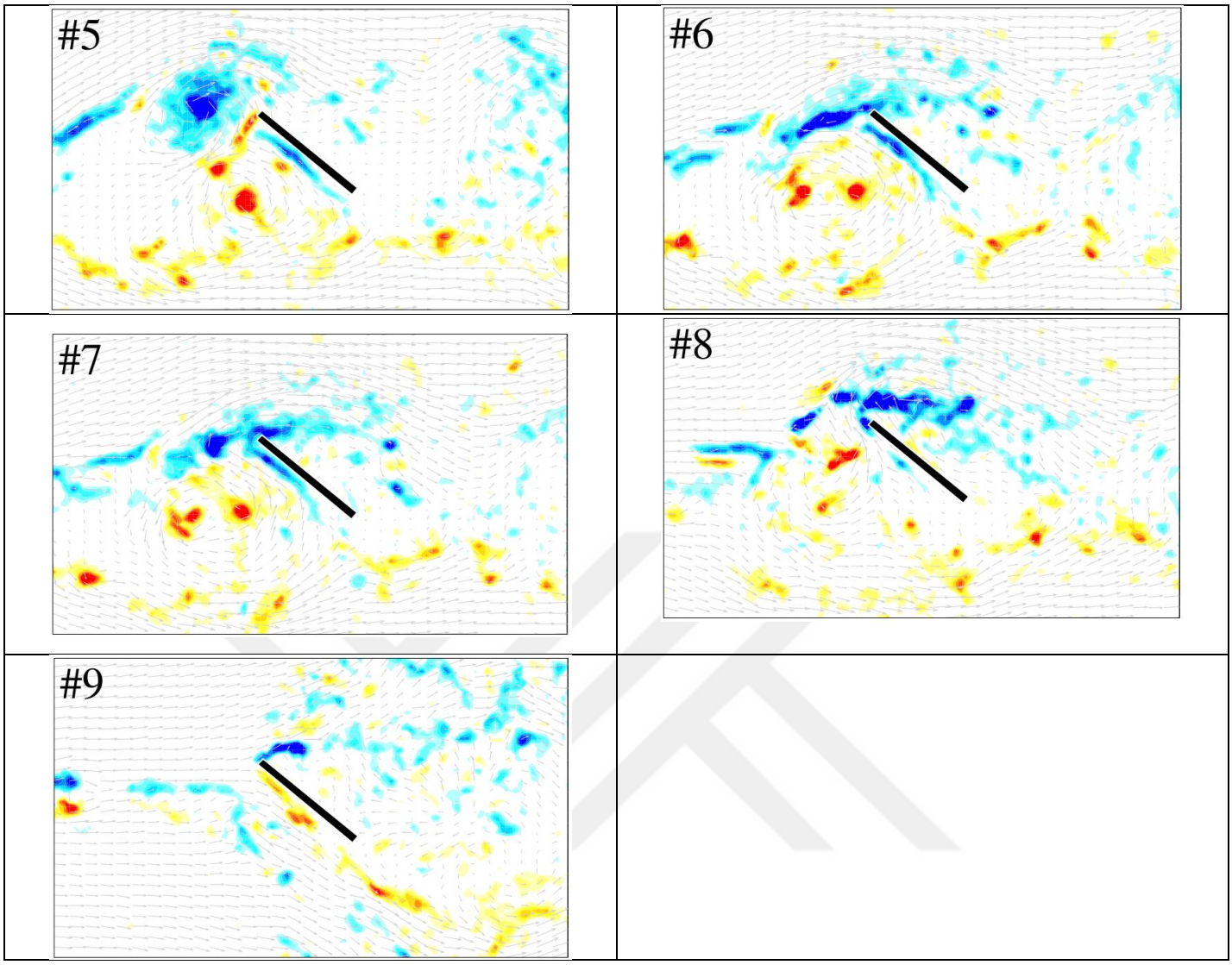

The gust generator vertical distance between the downstream flat plat has changed to understand the effect of LESP with different gust interactions on experiment 5. As it can be seen in table 4.3, the changing gust interaction did not change behaviour of LESP. However, on the 5th and the 6th images, the counterrotating votrex remains stayed on the airfoil as the clockwise leading-edge vortex occupy on the flat plate as the LESP equal to the negative amd the positive critical number. Theoretically LESP parameter state the circularity summation around the leading edge [14]. Consequently, the comparison between the PIV circularity calculation and the LESP from the force vector might give more about the LESP parameter itself.

Table 4.4: Force graph and the DPIV images of experiment 5

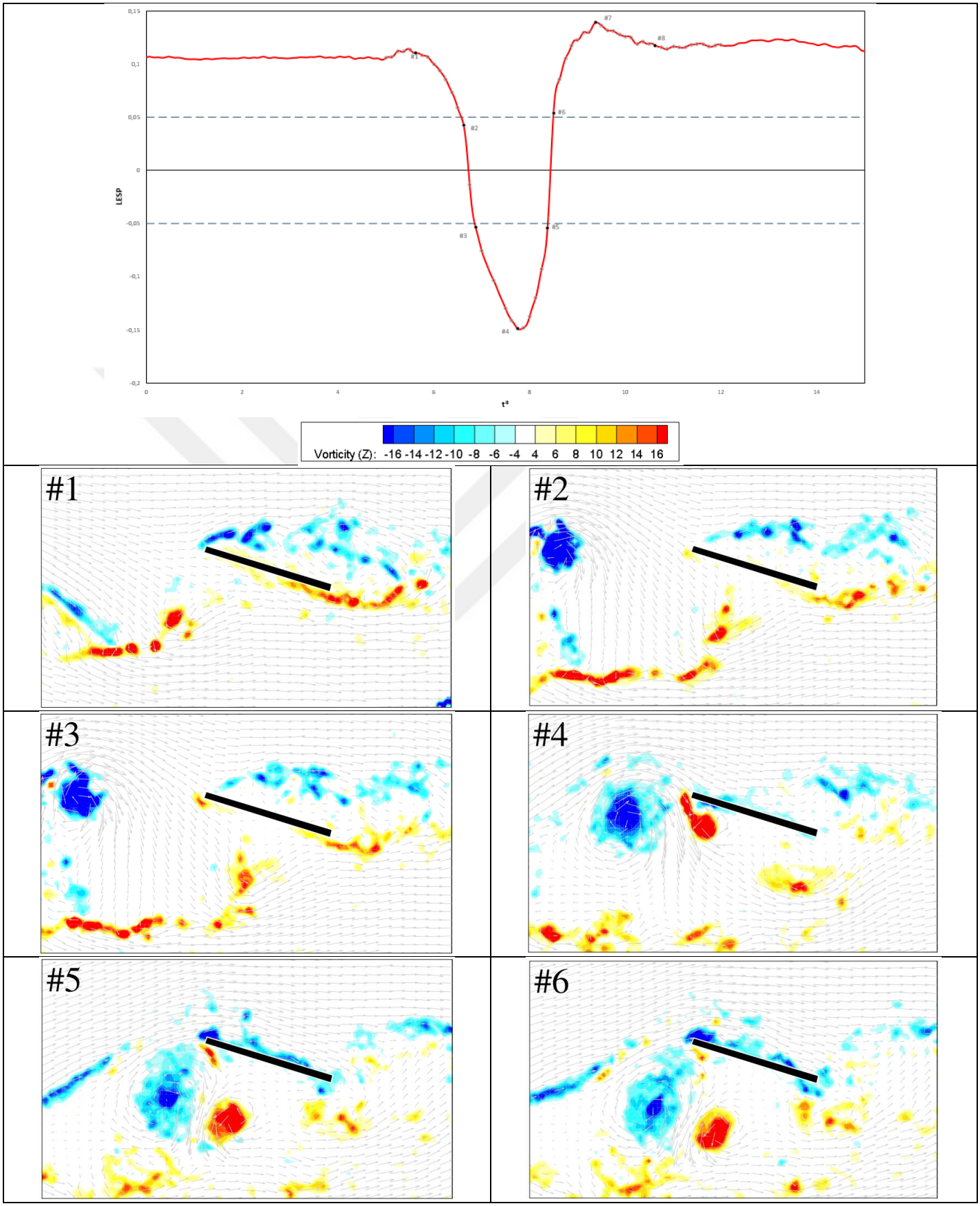

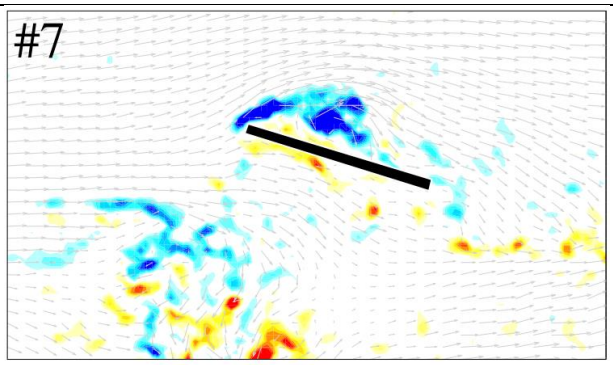
#7

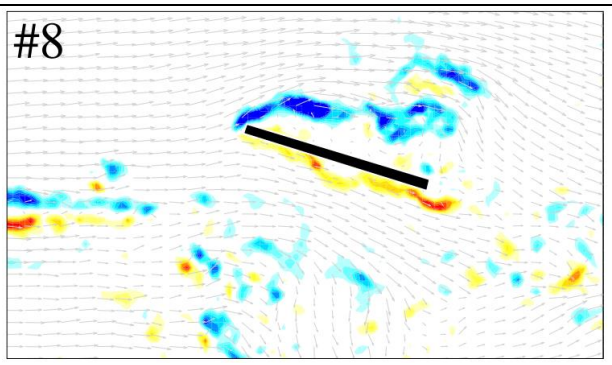
#8

6. CONCLUSIONS AND FUTURE WORK

In this study, the LESP hypothesis is investigated in a gust flow environment and the LESP parameter calculated as a function of the y vector of the force sensor. A different angle of attack and different gust impingement combination has been shown that the LESP parameter works even in a highly unstable gust environment. Flow structures around the airfoil leading edge are captured by the DPIV system while the force sensor acquiring the simultaneous measurement and DPIV images also showed that the flow structures around the flat plate are behaving as expected from the LESP theory (leading edge vortex separation and unification).

As future work, the same theory could be run with different airfoils rather than a flat plate. Theory suggests that even though every airfoil will have a different critical LESP number, leading edge behavior should be the same at the critical LESP number. In literature, different types of airfoil motion (plunge pitch) have been studied to show LESP work also this king of movements; however, it could be interesting to investigate gust and airfoil motion combine in terms of LESP. As a theory, LESP comes from the circulation radius of the flow around the leading edge; consequently, the circulation calculation at the leading edge from the PIV could explain better the critical LESP number and its variation in time.

REFERENCES

1] **Ellington, C., Van Den Berg, C., Willmott, A., and Thomas, A.,** "Leading-edge vortices in insect flight," *Nature*, Vol. 384, 1996, pp. 626–630.

2] **Shyy, W. and Liu, H.,** "Flapping Wings and Aerodynamic Lift: The Role of Leading-Edge Vortices," *AIAA journal*, Vol. 45, No. 12, 2007.

3] **Ellington, C.,** "The novel aerodynamics of insect flight: applications to micro-air vehicles," *Journal of Experimental Biology*, Vol. 202, No. 23, 1999, pp. 3439–3448.

4] **Dickinson, M. and Gotz, K.,** "Unsteady aerodynamic performance of model wings at low Reynolds numbers," *Journal of Experimental Biology*, Vol. 174, No. 1, 1993, pp. 45–64.

5] **Theodorsen, T.,** "General Theory of Aerodynamic Instability and the Mechanism of Flutter," NACA Rept. 496, 1935.

6] **Wagner, H.,** "Uber die Entstehung des dynamischen Auftriebes von Tragfl¨ugeln," ¨ *ZaMM* , Vol. 5, No. 1, 1925, pp. 17–35.

7] **McCroskey, W.,** "The phenomenon of dynamic stall." NASA TM-81264, 1981.

8] **Leishman, J. and Beddoes, T.,** "A Semi-Empirical Model for Dynamic Stall," Journal of the American Helicopter Society, Vol. 34, 1989, pp. 3–17.

9] **Beddoes, T. S.** "Onset of leading-edge separation effects under dynamic conditions and low Mach number" Proceedings ofthe 34th Annual Forum of the American Helicopter Society, 1978

10] **Garrick, I. E.** "Propulsion of a flapping and oscillating airfoil" Tech. rep. NACA Report No. 567, 1936

11] **Evans, W. and Mort, K.** "Analysis of computed ow parameters for a set of sudden stalls in low-speed two-dimensional flow" Tech. rep. NACA TN D-85, 1959

12] **Ramesh, K., Gopalarathnam, A., Ol, M. V. M., Granlund, K. and Edwards, J. R. J.** "Augmentation of inviscid airfoil theory to predict and model 2d unsteady vortex dominated flows" 41st AIAA Fluid Dynamics Conference, Vol 919, pp 115, 2011

13] **Ramesh, K., Gopalarathnam, A., Granlund, K., Ol, M. V. and Edwards, J. R.** "Discrete-vortex method with novel shedding criterion for unsteady aerofoil flows with intermittent leading-edge vortex shedding" Journal of Fluid Mechanics, Vol 751, pp 500-538, 2014

14] **Eldredge, J. D.,** "Mathematical Modeling of Unsteady Inviscid Flows, Interdisciplinary Applied Mathematics", Vol. 50, Springer International Publishing, 2019

15] **Ramesh, K., Gopalarathnam, A., Edwards, J.R., Ol, M.V., Granlund, K.:** "An unsteady airfoil theory applied to pitching motions validated against experiment and computation" Theor. Comput. Fluid Dyn. 27(6), pp 843–864 ,2013

16] **GARRICK, I.** "Propulsion of a flapping and oscillating aerofoil". *NACA Rep.* 567, 1937

17] **Von Karman, T. & Burgers, J. M.** "General Aerodynamic Theory – Perfect Fluids (ed. W. F. Durand)", Aerodynamic Theory: A General Review of Progress, vol. 2. Dover, 1963

18] **Polhamus, E. C.** "A concept of the vortex lift of sharp-edge delta wings based on a leading edge-suction analogy". NASA Tech. Rep. TN D-3767, 1966

19] **Fenercioglu, I.** "Experimental Investigation of Flow Structures Around an Oscillating Airfoil in Steady Current", *Ph.D. thesis*, Istanbul Technical University, 2010

20] **Fenercioglu, I. and Cetiner, O.** "Categorization of flow structures around a pitching and plunging airfoil" *Journal of Fluids and Structures*, *31*, 92–102, 2012

21] **Fenercioglu, I. and Cetiner, O.** "Effect of unequal flapping frequencies on flow structures", *Aerospace Science and Technology*, *35*, 39–53, 2014

22] **Engin, K.** "Experimental Investigation of a Single Spanwise Vortex Gust Impinging on a Rectangular Wing", *Msc thesis*, Istanbul Technical University, 2020

23] **He, G., Deparday, J., Siegel, L., Henning, A., and Mulleners, K.,** "Stall Delay and Leading-Edge Suction for a Pitching Airfoil with Trailing-Edge Flap," AIAA Journal, 2020

CURRICULUM VITAE

Name Surname **:** Egemen AYDIN

EDUCATION **:**

- **B.Sc.** **:**

PROFESSIONAL EXPERIENCE AND REWARDS:

PUBLICATIONS, PRESENTATIONS AND PATENTS ON THE THESIS: